A study of transient flows of Newtonian fluids through micro-annuals with a slip boundary

2009 J. Phys. A: Math. Theor. 42 065206

(http://iopscience.iop.org/1751-8121/42/6/065206)

IOP PUBLISHING JOURNAL OF PHYSICS A: MATHEMATICAL AND THEORETICAL

J. Phys. A: Math. Theor. **42** (2009) 065206 (14pp) doi:10.1088/1751-8113/42/6/065206

A study of transient flows of Newtonian fluids through micro-annuals with a slip boundary

B Wiwatanapataphee[1], Yong Hong Wu[2], Maobin Hu[3] and K Chayantrakom[2]

[1] Faculty of Science, Mahidol University, Bangkok 10400, Thailand
[2] Department of Mathematics and Statistics, Curtin University of Technology, Perth, WA 6845, Australia
[3] School of Engineering Science, University of Science and Technology of China, People's Republic of China

Received 8 August 2008, in final form 5 December 2008
Published 14 January 2009
Online at stacks.iop.org/JPhysA/42/065206

Abstract

In this paper, we study the pressure gradient driven transient flow of an incompressible Newtonian liquid in micro-annuals under a Navier slip boundary condition. By using the Fourier series expansion in time and Bessel functions in space, an exact solution is derived and is shown to include some existing known results as special cases. By analysing the exact solution, it is found that the influences of boundary slip on the flow behaviour are qualitatively different for different types of pressure fields driving the flow. For pressure fields with a constant pressure gradient, the flow rate increases with the increase in the slip parameter l almost linearly when l is large; while, for pressure fields with a wave form pressure gradient within a certain frequency range, as the slip parameter l increases, the amplitude of the flow rate increases first and then approaches a constant value when l becomes sufficiently large. It is also found that to achieve a given flow rate, one could have different designs and the graphs for the design are presented and discussed in this paper.

PACS numbers: 47.15.Rq, 47.60.Dx

1. Introduction

Recent advances in nanotechnologies have led to the development of many biological and engineering devices and systems in micro and nanoscales [18], such as biochemical lab-on-the-chip systems, micro-electromechanical systems, fuel cell devices, drug delivery systems [30], biological sensing and energy conversion devices [23]. Most of these devices and systems involve fluid flow through microchannels, referred to as microflows [2, 12, 14, 15]. As the behaviour of the fluid flow in these systems determines the functional characteristics of the systems, it is extremely important to study the mechanism of microflows so as to develop a better understanding [1, 11, 35].

From the fundamental principles of continuum mechanics, the flow of incompressible Newtonian fluids is governed by the continuity equation, the Navier–Stokes equations and a set of boundary conditions. Traditionally the so-called no-slip boundary condition is used, namely the fluid velocity relative to the solid is assumed to be zero on the fluid–solid interface [29]. However, evidences of slip of a fluid on a solid surface have been reported [25]. Chauveteau [7], Tuinier and Taniguchi [34], and Vargas and Manero [9] studied the flow of polymer solutions in porous media and showed that the apparent viscosity of the fluids near the wall is lower than that in the bulk and consequently the fluids can exhibit the phenomenon of apparent slip on the wall. More recently, experiments in micrometer scale and molecular dynamic simulations have shown that the flow of fluids in microsystems is granular and slip can occur on the fluid–solid interface [3, 4, 31, 40, 45]. Hence, under certain conditions such as those investigated in [33, 35], the no-slip condition is not acceptable for fluid flows in microchannels. On the other hand, many experimental results have provided evidences to support the Navier slip condition [16, 25, 42], namely the fluid velocity component tangential to the solid surface, relative to the solid surface, is proportional to the shear stress on the fluid–solid interface. The proportionality is called the slip length which describes the *slipperiness* of the surface [19, 42]. Some attempts have also been made to derive alternative formulae for the determination of the slip length [32], and to use nanotechnologies for the surface treatment of microchannels so as to achieve large slip for maximizing the transport efficiency of fluids through microchannels. Based on the nature of boundary slip of microflows, we will use the Navier slip condition for the fluid flow in micro-annuals.

Over the last couple of decades, many investigations have been made to study various flow problems of Newtonian and non-Newtonian fluids with the no-slip boundary condition or a slip boundary condition [5, 8, 10, 20, 21, 24, 27, 28, 43, 44]. Although exact and numerical solutions to many flow problems of Newtonian fluids under the no-slip assumption have been obtained and are available in the literature [29, 36–38], very few exact solutions for the slip case are available in the literature. Recently, some steady-state slip solutions for the flows through a pipe, a channel and an annulus have been obtained [22, 41]. An exact solution for the transient flow through microtubes has also been derived and discussed in the paper [39].

Motivated by the previous work, we study the transient flow of an incompressible Newtonian liquid through a micro-annual with a slip boundary in this paper. The work is basically an extension of our previous work in [39]. Here we should address that micro-devices with annulus geometry, such as microreactor with multicylindrical mixer structure [13], are extremely difficult to fabricate using current microfabrication technology. The rest of this paper is organized as follows. In the following section, we first define the problem and then present its mathematical formulation. In section 3, we solve the underlying boundary value problem to derive the exact solution for the velocity field and show that the solution includes some existing known solutions as special cases. In section 4, we derive exact solutions for the flow rate, the rate of deformation tensor and the stress field in the fluid using the exact solution of the velocity field derived in section 3. In section 5, an analysis is carried out to study the influence of the slip parameter on the flow behaviour. Finally, a conclusion is given in section 6.

2. Mathematical formulation

Consider the transient flow of an incompressible Newtonian liquid through a circular annual of inner radius a and outer radius R with the z-axis being in the axial direction as shown in figure 1. We limit our analysis to fully developed flow and assume that the slip length does not change along the flow. The field equations governing the flow include the continuity equation

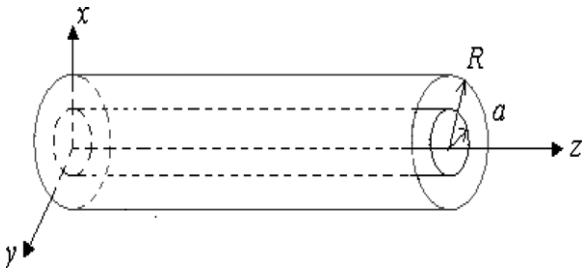

Figure 1. The coordinate system used.

and the Navier–Stokes equations. As the flow is axially symmetric and fully developed, there is no swirling flow and the velocity components in the radial and transverse directions vanish, namely $\mathbf{v} = (v_r, v_\theta, v_z) = (0, 0, u)$. Thus, from the continuity equation and the Navier–Stokes equations, as shown in [39], u must satisfy the following equation:

$$\frac{\mu}{\rho}\left(\frac{\partial^2 u}{\partial r^2} + \frac{1}{r}\frac{\partial u}{\partial r}\right) - \frac{\partial u}{\partial t} = \frac{1}{\rho}\frac{\partial p}{\partial z}. \tag{1}$$

Since a wide range of functions can be expressed in terms of Fourier series, in this work, we consider the fluid flow driven by the pressure field with a pressure gradient that can be expressed by the Fourier series

$$\frac{\partial p}{\partial z} = a_0 + \sum_{n=1}^{\infty}[a_n \cos(n\omega t) + b_n \sin(n\omega t)] := q(t). \tag{2}$$

To completely define the problem, the field equations must be supplemented by the boundary condition. In this work, we use the Navier slip boundary condition. That is, on the solid–fluid interfaces $r = a$ (inner surface) and $r = R$ (outer surface), the axial fluid velocity, relative to the solid surface, is proportional to the shear stress on the interface. For Newtonian fluids, the shear stress is related to the shear strain rate by $\sigma_{rz} = \mu\frac{\partial u}{\partial z}$ where μ is the fluid viscosity. Thus, for the case where the rigid micro-annulus is fixed spatially, the Navier slip condition can be written in the form of

$$u(a, t) = \pm l_1 \frac{\partial u}{\partial r}(a, t), \qquad u(R, t) = \pm l_2 \frac{\partial u}{\partial r}(R, t) \tag{3}$$

where l_1 and l_2 denote the slip parameters of the inner surface and the outer surface, respectively. In this study, we assume that the slip parameter does not change along the flow. The signs for the terms on the right-hand sides of the above equations have been discussed by various authors. In the literature, all the four possible cases are considered and the physically feasible cases are determined based on the solution derived. Here, we give a different method for choosing the sign for the terms on the right-hand sides of the equations in (3) without the need for finding the solution first, as detailed below.

From the physics of fluids, when the fluid moves relative to the solid surface in the tangential direction of the solid surface, the relative movement of the fluid particles will be restricted by a resistance force acting on the opposite direction of the relative movement. Let the unit outward normal vector of the surface S of the fluid be $\mathbf{n} = (n_1, n_2, n_3)$, and the positive tangential direction be $\mathbf{t} = (t_1, t_2, t_3)$. Suppose the stress tensor in the fluid is σ_{ij}, then the surface traction on S is $X_i = \sigma_{ji} n_j$ which has the tangential component $f_t = X_i t_i = \sigma_{ji} n_j t_i$, where we have used the index notation with the repeated literal indices representing summation

over the index range. On the other hand, the velocity component of the fluid relative to the solid surface in the tangential direction is $v_t - v_{st} = (v_i - v_{si})t_i$. Hence the Navier-type boundary condition for Newtonian fluids can be written as

$$v_t - v_{st} = -\frac{lf_t}{\mu} \qquad \text{or} \qquad (v_i - v_{si})t_i = -\frac{l(\sigma_{ji}n_j t_i)}{\mu}. \tag{4}$$

The negative sign in the above equations is to indicate that the direction of the relative tangential velocity is opposite to the surface traction force exerted on the fluid by the solid surface. Now for our problem in the (r, θ, z) system, $\mathbf{v} = (0, 0, u)$, $\mathbf{v}_s = (0, 0, 0)$. For the outer surface $r = R$, $\mathbf{n} = (1, 0, 0)$ and $\mathbf{t} = (0, 0, 1)$, and so $v_t - v_{st} = v_i t_i = u$ and $f_t = \sigma_{rz} = \mu\frac{\partial u}{\partial r}$ and consequently $(3)_2$ for the outer surface takes the following form:

$$u(R, t) = -l_2\frac{\partial u}{\partial r}(R, t). \tag{5}$$

For the inner surface $r = a$, $\mathbf{n} = (-1, 0, 0)$ and $\mathbf{t} = (0, 0, 1)$, and so $v_t - v_{st} = v_i t_i = u$ and $f_t = -\sigma_{rz} = -\mu\frac{\partial u}{\partial r}$ and consequently $(3)_1$ for the inner surface takes the following form:

$$u(a, t) = l_1\frac{\partial u}{\partial r}(a, t). \tag{6}$$

It should also be addressed here that for $l_i = 0$, conditions (5)–(6) reduce to the no-slip boundary condition; while, for $l_i \to \infty$, equations (5) and (6) give the surface traction condition for perfectly smooth surfaces, i.e., $\sigma_{rz}(a, t) = \sigma_{rz}(R, t) = 0$.

Remark 2.1. Formula (4) is more precise than (3) and is more suitable for application in numerical analysis.

3. Exact solution for the transient velocity field

To solve equation (1), first we use a complex number to express the above Fourier series by exponential functions, namely

$$\frac{\partial p}{\partial z} = \mathrm{Re}\left(\sum_{n=0}^{\infty} c_n \mathrm{e}^{\mathrm{i}n\omega t}\right) \tag{7}$$

where $c_n = a_n - b_n\mathrm{i}$ and $\mathrm{e}^{\mathrm{i}n\omega t} = \cos(n\omega t) + \mathrm{i}\sin(n\omega t)$.

From the linear property of equation (1), we have $u = \sum_{n=0}^{\infty}\mathrm{Re}(u_n)$, where u_n is defined by

$$\frac{\mu}{\rho}\left(\frac{\partial^2 u_n}{\partial r^2} + \frac{1}{r}\frac{\partial u_n}{\partial r}\right) - \frac{\partial u_n}{\partial t} = \frac{c_n}{\rho}\,\mathrm{e}^{\mathrm{i}n\omega t}. \tag{8}$$

As in [39], let

$$u_n = f_n(r)\,\mathrm{e}^{\mathrm{i}n\omega t}. \tag{9}$$

Then, we have

$$\frac{\mu}{\rho}\left(\frac{\partial^2 f_n}{\partial r^2} + \frac{1}{r}\frac{\partial f_n}{\partial r}\right) - \mathrm{i}n\omega f_n = \frac{c_n}{\rho}. \tag{10}$$

For $n = 0$, equation (10) has the following general solution:

$$f_0(r) = (A_1 + A_2\ln r) + \frac{c_0}{4\mu}r^2. \tag{11}$$

For $n \geqslant 1$, equation (10) can be written as

$$\bar{r}^2 \frac{\partial^2 f_n}{\partial \bar{r}^2} + \bar{r} \frac{\partial f_n}{\partial \bar{r}} + \bar{r}^2 f_n = \frac{c_n}{\beta_n^2 \mu} \bar{r}^2, \tag{12}$$

where $\beta_n^2 = n\beta^2$ in which $\beta^2 = -\frac{\rho\omega}{\mu}\mathrm{i}$, and $\bar{r} = \beta_n r$.

As the associated homogeneous equation is the zero-order Bessel equation, equation (12) has the following general solution:

$$f_n = d_n J_0(\bar{r}) + e_n Y_0(\bar{r}) + \frac{c_n}{\beta_n^2 \mu} = d_n J_0(\beta_n r) + e_n Y_0(\beta_n r) + \frac{c_n \mathrm{i}}{\rho n \omega}, \tag{13}$$

where d_n and e_n are integration constants; J_0 and Y_0 denote the zero-order Bessel functions of the first and second kinds, respectively. Thus, we have

$$u = \sum_{n=0}^{\infty} \mathrm{Re}(u_n) = A_1 + A_2 \ln(r) + \frac{a_0}{4\mu} r^2 + \sum_{n=1}^{\infty} \mathrm{Re}\left[\left(d_n J_0(\beta_n r) + e_n Y_0(\beta_n r) + \frac{c_n \mathrm{i}}{\rho n \omega} \right) \mathrm{e}^{\mathrm{i}n\omega t} \right], \tag{14}$$

from which we obtain

$$\frac{\partial u}{\partial r} = A_2 \frac{1}{r} + \frac{a_0}{2\mu} r - \mathrm{Re} \sum_{n=1}^{\infty} [d_n J_1(\beta_n r) + e_n Y_1(\beta_n r)] \beta_n \, \mathrm{e}^{\mathrm{i}n\omega t} \tag{15}$$

where, in the above formulation, we have used the identities

$$\frac{\mathrm{d}J_0(x)}{\mathrm{d}x} = -J_1(x), \qquad \frac{\mathrm{d}Y_0(x)}{\mathrm{d}x} = -Y_1(x). \tag{16}$$

Substituting (14) and (15) into the boundary conditions (5), (6) yields

$$\begin{aligned}
&\left(A_1 + A_2 \ln(a) + \frac{a_0}{4\mu} a^2 - A_2 \frac{1}{a} l_1 - \frac{a_0}{2\mu} a l_1 \right) + \mathrm{Re} \sum_{n=1}^{\infty} \Bigg[d_n J_0(\beta_n a) + e_n Y_0(\beta_n a) \\
&\qquad + \frac{c_n \mathrm{i}}{\rho n \omega} + l_1 \beta_n d_n J_1(\beta_n a) + l_1 \beta_n e_n Y_1(\beta_n a) \Bigg] \mathrm{e}^{\mathrm{i}n\omega t} = 0 \\
&\left(A_1 + A_2 \ln(R) + \frac{a_0}{4\mu} R^2 + A_2 \frac{1}{R} l_2 + \frac{a_0}{2\mu} R l_2 \right) + \mathrm{Re} \sum_{n=1}^{\infty} \Bigg[d_n J_0(\beta_n R) + e_n Y_0(\beta_n R) \\
&\qquad + \frac{c_n \mathrm{i}}{\rho n \omega} - l_2 \beta_n d_n J_1(\beta_n R) - l_2 \beta_n e_n Y_1(\beta_n R) \Bigg] \mathrm{e}^{\mathrm{i}n\omega t} = 0.
\end{aligned} \tag{17}$$

For the above equations to hold for any instant of time t, we require that

$$\begin{aligned}
&A_1 + A_2 \left(\ln(a) - \frac{1}{a} l_1 \right) = -\frac{a_0}{4\mu} (a^2 - 2a l_1), \\
&A_1 + A_2 \left(\ln(R) + \frac{1}{R} l_2 \right) = -\frac{a_0}{4\mu} (R^2 + 2R l_2), \\
&d_n [J_0(\beta_n a) + l_1 \beta_n J_1(\beta_n a)] + e_n [Y_0(\beta_n a) + l_1 \beta_n Y_1(\beta_n a)] = -\frac{c_n \mathrm{i}}{\rho n \omega}, \\
&d_n [J_0(\beta_n R) - l_2 \beta_n J_1(\beta_n R)] + e_n [Y_0(\beta_n R) - l_2 \beta_n Y_1(\beta_n R)] = -\frac{c_n \mathrm{i}}{\rho n \omega}.
\end{aligned} \tag{18}$$

Solving the above system of equations for A_1, A_2, d_n and e_n, and then submitting them into (14), we obtain

$$u = -\frac{a_0 R^2}{4\mu}\left(1 - \left(\frac{r}{R}\right)^2 + \frac{2l_2}{R} + \frac{1 - \left(\frac{a}{R}\right)^2 + 2\left(\frac{l_2}{R} + \frac{al_1}{R^2}\right)}{\ln\frac{R}{a} + \frac{l_2}{R} + \frac{l_1}{a}}\left(\ln\frac{r}{R} - \frac{l_2}{R}\right)\right) - \operatorname{Re}\sum_{n=1}^{\infty}\frac{c_n \mathrm{i}\,\mathrm{e}^{\mathrm{i}n\omega t}}{\rho n\omega}\left\{\frac{N_1}{D}J_0(\beta_n r) + \frac{N_2}{D}Y_0(\beta_n r) - 1\right\} \tag{19}$$

where

$$N_1 = N_1(a, R, \beta_n, l_1, l_2) = Y_0(\beta_n R) - Y_0(\beta_n a) - [l_2 Y_1(\beta_n R) + l_1 Y_1(\beta_n a)]\beta_n,$$

$$N_2 = N_2(a, R, \beta_n, l_1, l_2) = J_0(\beta_n a) - J_0(\beta_n R) + [l_1 J_1(\beta_n a) + l_2 J_1(\beta_n R)]\beta_n,$$

$$\begin{aligned} D = D(a, R, \beta_n, l_1, l_2) &= J_0(\beta_n a)Y_0(\beta_n R) - J_0(\beta_n R)Y_0(\beta_n a) \\ &+ [J_1(\beta_n a)Y_0(\beta_n R) - J_0(\beta_n R)Y_1(\beta_n a)]l_1\beta_n \\ &+ [J_1(\beta_n R)Y_0(\beta_n a) - J_0(\beta_n a)Y_1(\beta_n R)]l_2\beta_n \\ &+ [J_1(\beta_n R)Y_1(\beta_n a) - J_1(\beta_n a)Y_1(\beta_n R)]l_1 l_2\beta_n^2. \end{aligned} \tag{20}$$

Remark 3.1. If $l_1 = l_2 = 0$, solution (19) becomes

$$u = -\frac{a_0 R^2}{4\mu}\left\{1 - \left(\frac{r}{R}\right)^2 + \left[1 - \left(\frac{a}{R}\right)^2\right]\frac{\ln(r/R)}{\ln(R/a)}\right\} - \operatorname{Re}\sum_{n=1}^{\infty}\frac{c_n i\,\mathrm{e}^{\mathrm{i}n\omega t}}{\rho n\omega} \times \left\{\frac{[Y_0(\beta_n R) - Y_0(\beta_n a)]J_0(\beta_n r) + [J_0(\beta_n a) - J_0(\beta_n R)]Y_0(\beta_n r)}{J_0(\beta_n a)Y_0(\beta_n R) - J_0(\beta_n R)Y_0(\beta_n a)} - 1\right\} \tag{21}$$

which is the solution for the traditional no-slip case [17].

Remark 3.2. If $a_0 = -A \in R$, $c_n = 0$ for all $n \geqslant 1$, $l_1/R = l_2/R = l$, $a = \kappa R$, $u = -v_z\frac{a_0 R^2}{4\mu}$ then the solution reduces to a recent result given in equation (19) in [22].

4. Exact solution of the flow rate and the stress field

From the axial velocity solution (19), the flow rate can be determined as

$$Q(t) = \int_a^R 2\pi r u(r, t)\,\mathrm{d}r = Q_0 + \sum_{n=1}^{\infty} Q_n, \tag{22}$$

where Q_0 and Q_n are, respectively, the flow rate corresponding to the constant component and the nth harmonic component of the pressure gradient and

$$Q_0 = -\frac{a_0\pi R^4}{8\mu}\left\{\left[1 - \left(\frac{a}{R}\right)^2\right]\left[1 - \left(\frac{a}{R}\right)^2 + \frac{4l_2}{R}\right] - \frac{1 - \left(\frac{a}{R}\right)^2 + 2\left(\frac{l_2}{R} + \frac{al_1}{R^2}\right)}{\ln\frac{R}{a} + \frac{l_2}{R} + \frac{l_1}{a}} \times \left[1 - \left(\frac{a}{R}\right)^2 + \frac{2l_2}{R} - \frac{2l_2 a^2}{R^3} + 2\left(\frac{a}{R}\right)^2\ln\frac{a}{R}\right]\right\}, \tag{23}$$

$$Q_n = -\operatorname{Re}\left\{\left[\frac{N_1}{D}\int_a^R r J_0(\beta_n r)\,\mathrm{d}r + \frac{N_2}{D}\int_a^R r Y_0(\beta_n r)\,\mathrm{d}r - \frac{1}{2}(R^2 - a^2)\right]\frac{2\pi c_n \mathrm{i}\,\mathrm{e}^{\mathrm{i}n\omega t}}{n\rho\omega}\right\}. \tag{24}$$

From the identities

$$\frac{\mathrm{d}}{\mathrm{d}x}[xJ_1(x)] = xJ_0(x), \qquad \frac{\mathrm{d}}{\mathrm{d}x}[xY_1(x)] = xY_0(x), \tag{25}$$

we have

$$\begin{aligned}\int_a^R rJ_0(\beta_n r)\mathrm{d}r &= \frac{1}{\beta_n}[RJ_1(\beta_n R) - aJ_1(\beta_n a)],\\ \int_a^R rY_0(\beta_n r)\mathrm{d}r &= \frac{1}{\beta_n}[RY_1(\beta_n R) - aY_1(\beta_n a)].\end{aligned} \tag{26}$$

Thus, by substituting the above formula into (22), we have

$$\begin{aligned}Q_n = -\mathrm{Re}\,\frac{2\pi c_n \mathrm{i}\,\mathrm{e}^{\mathrm{i}n\omega t}}{n\rho\omega}\Bigg\{&\frac{N_1}{\beta_n D}[RJ_1(\beta_n R) - aJ_1(\beta_n a)]\\ &+\frac{N_2}{\beta_n D}[RY_1(\beta_n R) - aY_1(\beta_n a)] - \frac{1}{2}(R^2 - a^2)\Bigg\}.\end{aligned} \tag{27}$$

Remark 4.1. From the above solution form, it is not immediately clear whether the transient flow rate increases as l_1 and/or l_2 increases, and thus we will study this in section 5.

The stress in the fluid is related to the velocity field by the following constitutive equations:

$$\sigma = -pI + 2\mu\,\mathbf{d}, \tag{28}$$

while the rate of the deformation tensor is related to the velocity vector by

$$\mathbf{d} = \tfrac{1}{2}(\nabla\mathbf{v} + (\nabla\mathbf{v})^T), \tag{29}$$

where $\sigma \equiv (\sigma_{ij})$ and $\mathbf{d} = (d_{ij})$ denote, respectively, the second-order stress tensor and the rate of the deformation tensor, I is an identity matrix. As $\mathbf{v} = (0, 0, u(r, t))$, we have

$$\mathbf{d} = \frac{1}{2}\begin{pmatrix} 0 & 0 & \partial u/\partial r\\ 0 & 0 & 0\\ \partial u/\partial r & 0 & 0\end{pmatrix}. \tag{30}$$

From the above formula and using (19), we obtain $d_{rr} = d_{\theta\theta} = d_{zz} = d_{r\theta} = d_{\theta z} = 0$ and

$$\begin{aligned}d_{rz} = -\frac{a_0 R}{8\mu}\left[-\frac{2r}{R} + \frac{1 - \left(\frac{a}{R}\right)^2 + 2\left(\frac{l_2}{R} + \frac{al_1}{R^2}\right)}{\ln\frac{R}{a} + \frac{l_2}{R} + \frac{l_1}{a}}\frac{R}{r}\right] + \mathrm{Re}\sum_{n=1}^{\infty}\frac{c_n \mathrm{i}\,\mathrm{e}^{\mathrm{i}n\omega t}}{2\rho n\omega}\\ \times\left\{\frac{N_1(a, R, \beta_n, l_1, l_2)}{D(a, R, \beta_n, l_1, l_2)}\beta_n J_1(\beta_n r) + \frac{N_2(a, R, \beta_n, l_1, l_2)}{D(a, R, \beta_n, l_1, l_2)}\beta_n Y_1(\beta_n r)\right\}.\end{aligned} \tag{31}$$

Hence from the constitutive equations (28), we obtain

$$\sigma_{rr} = \sigma_{\theta\theta} = \sigma_{zz} = -p = q(t)z + p_0(t), \qquad \sigma_{r\theta} = \sigma_{\theta z} = 0$$

$$\begin{aligned}\sigma_{rz} = -\frac{a_0 R}{4}\left[-\frac{2r}{R} + \frac{1 - \left(\frac{a}{R}\right)^2 + 2\left(\frac{l_2}{R} + \frac{al_1}{R^2}\right)}{\ln\frac{R}{a} + \frac{l_2}{R} + \frac{l_1}{a}}\frac{R}{r}\right] + \mathrm{Re}\sum_{n=1}^{\infty}\frac{c_n \mu \mathrm{i}\,\mathrm{e}^{\mathrm{i}n\omega t}}{\rho n\omega}\\ \times\left\{\frac{N_1(a, R, \beta_n, l_1, l_2)}{D(a, R, \beta_n, l_1, l_2)}\beta_n J_1(\beta_n r) + \frac{N_2(a, R, \beta_n, l_1, l_2)}{D(a, R, \beta_n, l_1, l_2)}\beta_n Y_1(\beta_n r)\right\}\end{aligned} \tag{32}$$

where $q(t)$ is as given in (2) while $p_0(t)$ is arbitrary and can be chosen to meet certain pressure conditions.

5. Discussions of the influence of boundary slip on the flow behaviour

With the exact solutions obtained in the previous sections, in this section, we discuss the influences of the slip length on velocity, flow rate and stresses in the fluid. As the solution for a general pressure field given by (2) is the superposition of the solution due to the constant pressure gradient and the solutions due to the sine and cosine wave form pressure gradients, without loss of generality, we consider here two different cases of driving pressure fields in this discussion. The first case is for a pressure field with a constant pressure gradient, while the second one is for a pressure field with a sine wave form pressure gradient. For convenience in the discussion, we introduce the following dimensionless variables:

$$r^* = \frac{r}{R}, \qquad k = \frac{a}{R}, \qquad l = \frac{l_2}{R}, \qquad \lambda = \frac{l_1}{l_2}, \qquad t^* = \frac{\omega t}{2\pi}, \qquad \beta^* = \beta R. \tag{33}$$

Case 1: $\frac{\mathrm{d}p}{\mathrm{d}z} = a_0$. For this case, $c_n = 0$ for all $n \geqslant 1$. Then from (19), (22)–(23) and (32), we obtain the following normalized velocity, normalized flow rate and shear stress:

$$u^* = -\frac{4\mu}{a_0 R^2} u = \left[1 - r^{*2} + 2l + \frac{1 - k^2 + 2(1 + k\lambda)l}{\ln \frac{1}{k} + \left(1 + \frac{\lambda}{k}\right) l} (\ln r^* - l) \right], \tag{34}$$

$$\begin{aligned} Q^* &= -\frac{8\mu}{a_0 \pi R^4} Q \\ &= (1 - k^2)(1 - k^2 + 4l) - \frac{1 - k^2 + 2(1 + k\lambda)l}{\ln \frac{1}{k} + \left(1 + \frac{\lambda}{k}\right) l} [(1 - k^2)(1 + 2l) + 2k^2 \ln(k)] \end{aligned} \tag{35}$$

$$\sigma^*_{rz} = -\frac{4}{a_0 R} \sigma_{rz} = \left[-2r^* + \frac{1 - k^2 + 2(1 + k\lambda)l}{\ln \frac{1}{k} + \left(1 + \frac{\lambda}{k}\right) l} \frac{1}{r^*} \right]. \tag{36}$$

It should be addressed here that for $l = 0$, the solution (34) reduces to the solution for the no-slip case [17]. To study the influence of l on the velocity, we examine the derivative of u^* with respect to l. From (34), we have

$$\frac{\mathrm{d}u^*}{\mathrm{d}l} = [a(k, \lambda, r^*) + b(k, \lambda)l + c(k, l)l^2] \left[\ln \frac{1}{k} + \left(1 + \frac{\lambda}{k}\right) l \right]^{-2}, \tag{37}$$

where

$$a(k, \lambda, r^*) = (2\ln(k) + 1 - k^2)(\ln(k) - \ln(r^*)) - \lambda k \ln(r^*) \left(2\ln(k) + \frac{1}{k^2} - 1 \right),$$

$$b(k, \lambda) = 4\lambda \ln(k) \left(k - \frac{1}{k} \right), \; c(k, \lambda) = 2\lambda \left(\frac{1}{k} - k \right) \left(1 + \frac{\lambda}{k} \right)$$

As $\lambda > 0, 0 < k < 1$, and $k \leqslant r^* \leqslant 1$, we can easily prove that $a > 0, b > 0$ and $c > 0$, and hence $\frac{\mathrm{d}u^*}{\mathrm{d}l} > 0$ for $l \geqslant 0$, which means that the velocity is a monotonically increasing function of l. Similarly, we can also prove that the flow rate also increases monotonically as l increases from zero. Also, for $l >> \max\left\{1, \ln \frac{1}{k}\right\}$, from (35), we have

$$\frac{\partial Q*}{\partial l} \approx 4(1 - k^2) \left(1 - \frac{1 + k\lambda}{1 + \lambda/k} \right) > 0$$

which indicates that Q^* increases almost linearly with increasing l when l is sufficiently large.

To further demonstrate the characteristics of the variation of the flow rate with l and k, we show the solution (35) graphically in figure 2 for the case where both the inner and outer surfaces have the same smoothness, i.e. $\lambda = 1$. The result shows that there exist different (l, k)

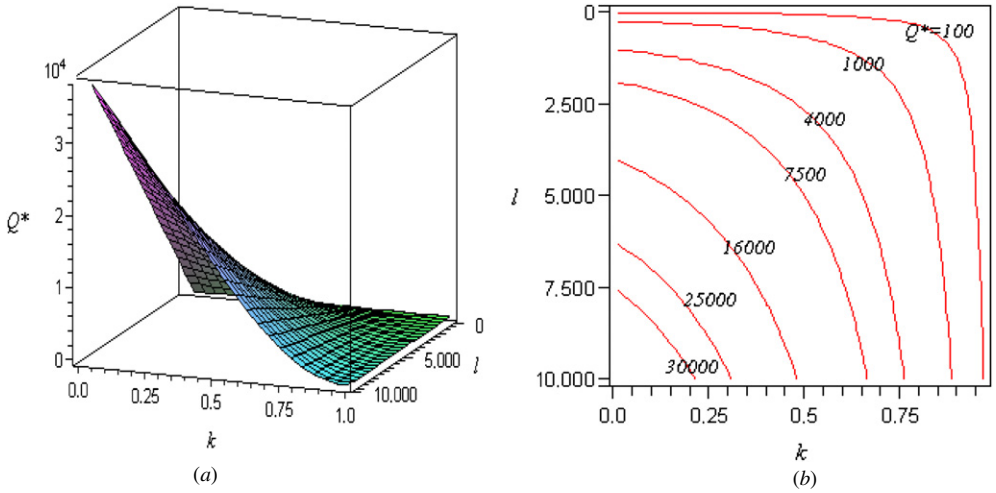

Figure 2. Variation of the flow rate with l and k obtained from solution (35) with $\lambda = 1$: (*a*) 3D graph for $Q^*(k, l)$; (*b*) contour plot of $Q^*(k, l)$ on the (k, l) plane.

parameter designs for obtaining a given fixed flow rate, which opens a way for the optimal design of the annual. The result also shows that the influence of l on the flow rate is more significant for lower k values. It is also interesting to note that the velocity field in the annual is not a simple superposition of the no-slip solution and a rigid body translation, as is in the circular microtubes [39].

Case 2: $\frac{\mathrm{d}p}{\mathrm{d}z} = b_1 \sin(\omega t)$. For this case, $a_0 = 0, c_1 = -b_1\mathrm{i}, c_n = 0$ for all $n \geqslant 2$. As $\beta^2 = -\frac{\rho\omega}{\mu}\mathrm{i} = \frac{\rho\omega}{\mu}\mathrm{e}^{-\pi\mathrm{i}/2}$, we have

$$\beta = \sqrt{\frac{\rho\omega}{2\mu}}(1-i) = \frac{\bar{\beta}}{R}(1-i), \qquad \frac{1}{\beta} = \frac{R}{2\bar{\beta}}(1+i), \qquad \beta^* = \bar{\beta}(1-i), \tag{38}$$

where $\bar{\beta} = R\sqrt{\frac{\rho\omega}{2\mu}}$ is a dimensionless parameter. Then, by using the dimensionless variables in (33), we have from (19), (27) and (32) that

$$\begin{aligned} u^* &= -\frac{\rho}{b_1}u \\ &= \mathrm{Re}\left\{\left[\frac{N_1}{D}J_0(\beta^* r^*) + \frac{N_2}{D}Y_0(\beta^* r^*) - 1\right]\frac{1}{\omega}\mathrm{e}^{2\pi t^*\mathrm{i}}\right\} \end{aligned} \tag{39}$$

$$\begin{aligned} Q^* &= -\frac{\rho}{2\pi b_1 R^2}Q_n \\ &= \mathrm{Re}\left\{\left[\frac{N_1}{\beta^* D}[J_1(\beta^*) - kJ_1(\beta^* k)] + \frac{N_2}{\beta^* D}[Y_1(\beta^*) - kY_1(\beta^* k)] - \frac{1}{2}(1-k^2)\right]\frac{1}{\omega}\mathrm{e}^{2\pi t^*\mathrm{i}}\right\} \end{aligned} \tag{40}$$

$$\begin{aligned} \sigma_{rz}^* &= \frac{\rho R}{\mu b_1}\sigma_{rz} \\ &= \mathrm{Re}\left\{\left[\frac{N_1}{D}\beta^* J_1(\beta^* r^*) + \frac{N_2}{D}\beta^* Y_1(\beta^* r^*)\right]\frac{1}{\omega}\mathrm{e}^{2\pi t^*\mathrm{i}}\right\} \end{aligned} \tag{41}$$

where

$$
\begin{aligned}
N_1 &= Y_0(\beta^*) - Y_0(\beta^* k) - [Y_1(\beta^*) + \lambda Y_1(\beta^* k)] l\beta^*, \\
N_2 &= J_0(\beta^* k) - J_0(\beta^*) + [\lambda J_1(\beta^* k) + J_1(\beta^*)] l\beta^*, \\
D &= J_0(\beta^* k) Y_0(\beta^*) - J_0(\beta^*) Y_0(\beta^* k) + [J_1(\beta^* k) Y_0(\beta^*) - J_0(\beta^*) Y_1(\beta^* k)] \lambda l\beta^* \\
&\quad + [J_1(\beta^*) Y_0(\beta^* k) - J_0(\beta^* k) Y_1(\beta^*)] l\beta^* \\
&\quad + [J_1(\beta^*) Y_1(\beta^* k) - J_1(\beta^* k) Y_1(\beta^*)] \lambda l^2 \beta^{*2}.
\end{aligned} \tag{42}
$$

For convenience in discussion, let

$$
\frac{N_1}{\omega\beta^* D}[J_1(\beta^*) - kJ_1(\beta^* k)] + \frac{N_2}{\omega\beta^* D}[Y_1(\beta^*) - kY_1(\beta^* k)] := a + b\mathrm{i}, \tag{43}
$$

then equation (40) can be written as

$$
Q^* = Q_m^*(k, l) \sin(2\pi t^* + \phi(k, l)),
$$

where $Q_m^*(k, l)$ and $\phi(k, l)$ are respectively the amplitude and phase angles of the normalized transient flow rate defined by

$$
\begin{aligned}
Q_m^*(k, l) &= \left(\left(a - \frac{1}{2\omega}(1 - k^2) \right)^2 + b^2 \right)^{1/2} \\
\phi(k, l) &= \arctan \left(\frac{\frac{1}{2\omega}(1 - k^2) - a}{b} \right).
\end{aligned} \tag{44}
$$

In the following, we first study the influence of the angular frequency ω on the amplitude of the transient flow rate $Q_m^*(k, l)$, and compare the transient solutions with the quasi steady-state solution which is obtained by neglecting the time derivative term in equation (1) to yield

$$
u^* = -\frac{\rho}{b_1} u = \frac{\rho R^2}{4\mu} \left[1 - r^{*2} + 2l + \frac{1 - k^2 + 2(1 + k\lambda)l}{\ln \frac{1}{k} + \left(1 + \frac{\lambda}{k}\right) l} (\ln r^* - l) \right] \sin(2\pi t^*) \tag{45}
$$

and

$$
\begin{aligned}
Q_s^* &= -\frac{\rho}{2\pi b_1 R^2} Q \\
&= \frac{\rho R^2}{16\mu} \left\{ (1 - k^2)(1 - k^2 + 4l) - \frac{1 - k^2 + 2(1 + k\lambda)l}{\ln \frac{1}{k} + (1 + \frac{\lambda}{k}) l} [(1 - k^2)(1 + 2l) + 2k^2 \ln(k)] \right\} \\
&\quad \times \sin(2\pi t^*).
\end{aligned} \tag{46}
$$

Figure 3 shows the influence of l on Q_m^* for a different angular frequency ω. Obviously, as the angular frequency decreases, the amplitude of the transient flow rate increases and the transient solution converges towards the quasi steady-state solution. It is also noted that the dependence of the amplitude of the transient flow rate on l is very different for different frequencies. At high frequency, the amplitude of the flow rate increases initially as l increases but tends to a constant value once l becomes sufficiently large. On the other hand, at low frequency the flow rate continues to increase with l and depends on l almost linearly for large l values.

Next, as an illustration, we investigate in more detail the influence of k and l on the flow rate for the frequency, $\omega = 5.0 \times 10^{-4} \mu/\rho R^2$, corresponding to a state that is not so close to the quasi steady state as shown in figure 3. We consider here the case where both the inner and outer surfaces have the same smoothness, i.e $\lambda = 1$. For this case, (44) gives the amplitude of the normalized flow rate as a function of the variables l and k which is shown graphically in figure 4. From the results, various findings can be obtained.

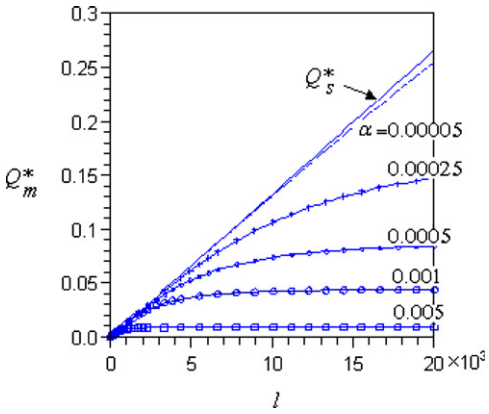

Figure 3. Influence of l on the quasi steady-state solution Q_s^* and the transient solution Q_m^* under different frequencies $\omega = \alpha\mu/\rho R^2$ with five different α values: $\alpha = 5.0 \times 10^{-3}$ (dash-box line), $\alpha = 1.0 \times 10^{-3}$ (dash-circle line), $\alpha = 5.0 \times 10^{-4}$ (dash-diamond line), $\alpha = 2.5 \times 10^{-4}$ (dash-cross line) and $\alpha = 5.0 \times 10^{-5}$ (dash line).

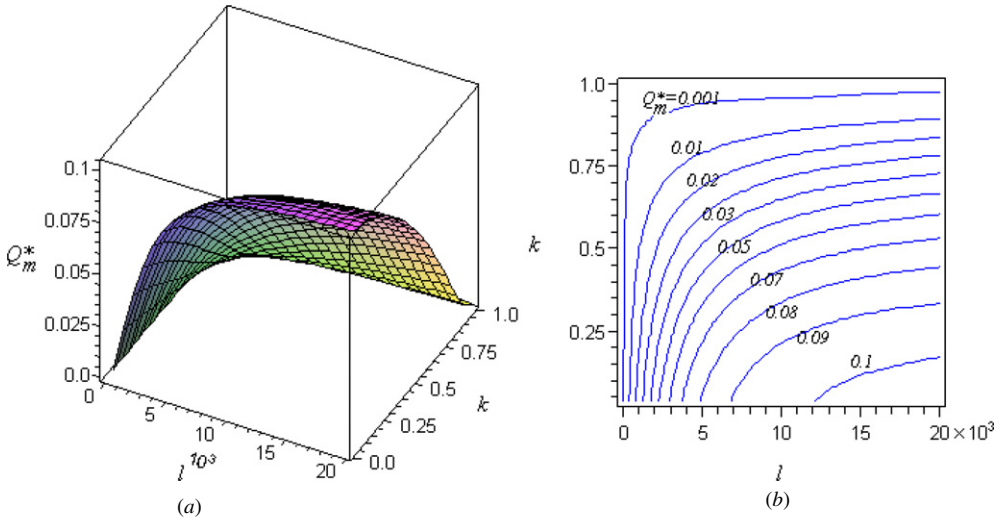

Figure 4. Variation of the amplitude of the flow rate with l and k obtained from solution (44) with $\lambda = 1$, $R = 1.0 \times 10^{-5}$, $\rho = 1060$, $\mu = 0.001$, $\omega = 5.0 \times 10^{-4}\mu/\rho R^2$: (*a*) 3D graph for Q_m^*, (*b*) contour plot of Q_m^* on the (k, l) plane.

(i) Unlike for the case of constant pressure gradient, the flow rate in this case no longer increases linearly with l for large l values. For each fixed k value, as l increases, the flow rate increases first and then tends to a constant once l becomes large. The critical l value at which the amplitude of the flow rate tends to a constant value decreases with the increase of the k value.

(ii) The amplitude of the flow rate decreases as k increases, as shown in figure 5. This is because the increase of k not only reduces the cross-section area for the fluid flow, but also leads to lower slip velocity on the solid surface as shown in figure 6.

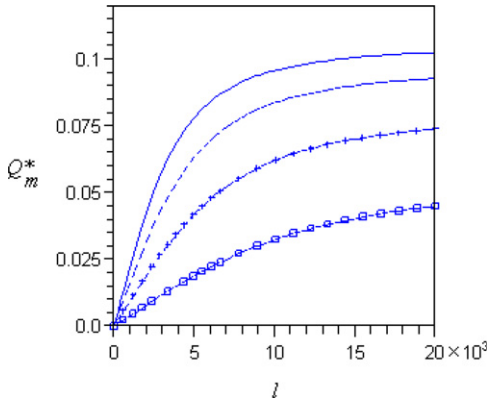

Figure 5. Variation of the amplitude of the flow rate with l for $\omega = 5.0 \times 10^{-4}\mu/\rho R^2$ and various different k values in case 2: $k = 0.1$ (solid line), $k = 0.3$ (dash line), $k = 0.5$ (dash-cross line), $k = 0.7$ (dash-box line).

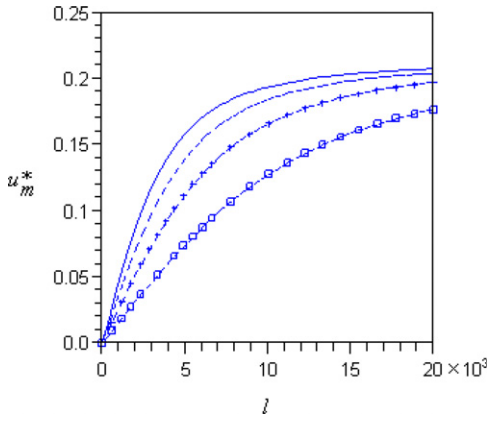

Figure 6. Variations of the amplitude of the slip velocity u_m^* on the outer surface $r^* = 1$ with l for $\omega = 5.0 \times 10^{-4}\mu/\rho R^2$ and various different k values in case 2: $k = 0.1$ (solid line), $k = 0.3$ (dash line), $k = 0.5$ (dash-cross line), $k = 0.7$ (dash-box line).

(iii) As for the constant case, one could have different (k, l) designs to achieve a given flow rate and figure 4(b) provides a tool for the design.

(iv) The influence of l on the flow rate becomes less and less significant as k increases.

6. Conclusions

In this paper, we derive the exact solutions for the pressure gradient driven transient flow of an incompressible Newtonian liquid through a circular annual with a Navier slip boundary. Based on the analytical expressions of the solutions, we analyse the influence of the slip parameter l and the geometry of the cross-section on the flow rate of fluid through the annual. The study shows that

(i) The influence of boundary slip on the flow through the annual is different for different types of pressure gradients. For flows driven by a constant pressure gradient, the flow rate always increases with the slip parameter l and achieves a linear increase rate for large l value; while, for the flows driven by the wave form pressure gradient with high frequency, the flow rate initially increases significantly as l increases from zero but tends to a constant when l becomes sufficiently large.

(ii) To achieve a fixed value of flow rate, one could have different (k, l) designs. The exact solutions obtained in this paper, together with the contour plots of the solutions (figure 2(b) and figure 4(b)), provide a tool for engineers and scientists to determine the proper (k, l) values.

Acknowledgments

The first author is grateful to the financial support of the Thailand Research Fund (TRF) and Mahidol University. The second author gratefully acknowledges the support of the Australian Research Council through a discovery project grant. The authors are also grateful to both referees for their comments and suggestions which have led to significant improvement of this paper.

References

[1] Arkilic E B, Schmidt M A and Breuer K S 1997 *Microelectromech. Syst.* **6** 167
[2] Bourlon B, Wong J and Miko C 2007 *Nature Nanotechnology* **2** 104
[3] Cao B Y, Chen M and Goo Z Y 2006 *Acta Phys. Sin.* **55** 5305
[4] Cao B Y, Chen M and Guo Z Y 2006 *Phys. Rev.* E **74** 066311
[5] Cai C, Sun Q and Boyd I D 2007 *Fluid Mech.* **589** 305
[6] Carpinlioglu M and Gundogdu M 2001 *Flow Meas. Instr.* **12** 163
[7] Chauveteau G 1982 *J. Rheol.* **26** 111
[8] Cosgrove J A, Buick J M, Tonge S J, Munro C G, Greated C A and Campbell D M 2003 *J. Phys. A : Math. Gen.* **36** 2609–20
[9] De Vargas L and Manero O 1989 *Polym. Eng. Sci.* **29** 1232
[10] Deshmukh S R and Vlachos D G 2005 *Indust.Eng. Chem. Res.* **44** 4982
[11] Gad-el-Hak M 1999 *Trans. ASME, J. Fluids Eng.* **121** 5
[12] Herwig H and Hausner O 2003 *Int. J. Heat Mass Transfer* **46** 935
[13] Hessel V, Knobloch C and Löwe H 2008 *Recent patents on Chem. Eng.* **1** 1–16
[14] Ho C M and Tai C Y 1998 *Annu. Rev. Fluid Mech.* **30** 579
[15] Huang H, Lee T S and Shu C 2007 *Int. J. Numer. Methods for Heat Fluid Flow* **17** 587
[16] Huang P and Breuer K S 2007 *Phys. Fluids* **19** 028104
[17] Hunter S C 1983 *Mechanics of Continuous Media* (New York: Wiley)
[18] Kuo T C, Cannon D M, Shannon M A, Bohn P W and Sweedler J V 2003 *Sensors Actuators* A **102** 223
[19] Lauga E and Squires T M 2005 *Phys. Fluids* **17** 103102
[20] Lee H B, Yeo I W and Lee K K 2007 *Geophys. Res. Lett.* **34** 19401
[21] Martin M J and Boyd I D 2006 *AIAA J Thermophys. Heat Transfer* **20** 710
[22] Matthews M T and Hill J M 2007 *Acta Mech.* **191** 195
[23] Nakane J J, Akeson M and Marziali A 2005 *J. Phys.: Condens. Matter* **15** R1365
[24] Pascal J P 2006 *J. Non-Newtonian Fluid Mech.* **133** 109
[25] Pit R, Hervet H and Leger L 2000 *Phys. Rev. letter* **85** 980
[26] Ray S, Unsal B, Durst F, Ertunc O and Bayoumi O A 2005 *Journal Fluids Eng.* **127** 405
[27] Sahu K C, Valluri P, Spelt P D M and Matar O K 2007 *Phys. Fluids* **19** 122101
[28] Saidi F 2006 *ZAMM-Zeitschrift fur Angewandte Mathematik und Mechanik* **86** 702
[29] Slattery J C 1999 *Advanced transport phenomena* (Cambridge: Cambridge University Press)
[30] Su Y C and Lin L W 2004 *J. Microelectromech. Syst.* **13** 75
[31] Szalmas L 2006 *Phys. Rev.* E **73** 066710
[32] Thompson P A and Troian S M 1997 *Nature* **389** 360

[33] Tretheway D C and Meinhart C D 2002 *Phys. Fluids* **14** L9
[34] Tuinier R and Taniguchi T 2005 *J. Phys.: Condens. Matter* **17** L9
[35] Yanuar K Watanabe and Mizunuma H 1998 *JSME Int. Journal Ser.* B **41** 525
[36] Wiwatanapataphee B, Wu Y H, Archapitak J, Siew P F and Unyong B 2004 *J. Comput. Appl. Math.* **166** 307
[37] Wiwatanapataphee B, Poltem D, Wu Y H and Lenbury Y 2006 *Math. Biosciences Eng.* **3** 371
[38] Wu Y H and Wiwatanapataphee B 2007 *Discrete and Continuous Dynamical Systems-Series* B **8** 695
[39] Wu Y H, Wiwatanapataphee B and Hu M 2008 *Physica* A **387** 5979–90
[40] Xu J L and Li Y X 2007 *Int. J. Heat Mass Transfer* **50** 2571–258
[41] Yang S P and Zhu K Q 2006 *J. Non-Newtonian Fluid Mech.* **138** 173
[42] Ybert C, Barentin C, Cottin-Bizonne C, Joseph P and Bocquet L 2007 *Phys. Fluids* **19** 123601
[43] You D and Moin P 2007 *Phys. Fluids* **19** 081701
[44] Yousif H A and Melka R 1997 *Comput. Phys. Commun.* **106** 199
[45] Zhu Y X and Granick S 2001 *Phys. Rev. Lett.* **87** 096105